6800 *Macromolecules* **2010**, *43*, 6800–6810
DOI: 10.1021/ma100642z

Macromolecules
ARTICLE

Determination of the Modulus of Thin Sol−Gel films Using Buckling Instability

Jonathan E. Longley* and Manoj K. Chaudhury

Department of Chemical Engineering, Lehigh University, Bethlehem, Pennsylvania 18015

Received March 25, 2010; Revised Manuscript Received June 9, 2010

ABSTRACT: Buckling instabilities have been used to estimate the elastic modulus of thin sol−gel films. The sol−gel films (65−400 nm) were coated on elastomeric supports, which were then subjected to a compressive strain imposed directly or as a result of thermal stresses generated during the curing cycle. Atomic force and optical microscopies were used to characterize the buckling wavelength, and electron microscopy was used to estimate the thickness of the films. Elastic modulus was calculated using the classical buckling theory. This procedure, which was demonstrated previously by others starting with the systematic studies of Stafford et al. (*Nature Mater*. **2004**, *3*, 545−550), proves to be an effective way of determining the elastic modulus of thin films. The technique is used to study the effects of the concentration of the chemical precursors, curing temperature, and the duration of cure and humidity on the moduli of sol−gel films, which provide valuable information about its performance when used as an adhesion promoter.

Introduction

Hybrid organic−inorganic thin films prepared using sol−gel processing are useful in such areas as adhesion promotion,[1,2] responsive coatings,[3] and corrosion resistance[4] technologies. Their popularity stems from the fact that they are easily processable in terms of dip, spin, or spray coatings and are curable at reasonably low temperature, i.e., below 150 °C. These sol−gel systems generally involve the reaction between silanes and metal alkoxides. The detailed chemistry of the formation of the sol−gel coating is, however, complex depending on the relative concentrations and types of the various constituents used to prepare them.[1,3,5,6] Predicting the effect of one of these parameters on the final film properties, such as modulus, porosity, and cross-link density, is not obvious. What would be ideal for further progress of these technologies is to develop methods that would allow rapid characterization of the properties of the thin film as a function of the various chemical and processing parameters. Estimation of elastic modulus is one such property that is intrinsically linked to the cross-link density and thus the extent to which the film is cured. Determination of the modulus of a sol−gel film is typically carried out via indentation methods.[7,8] However, a number of issues such as the effect of the support and their viscoelastic behavior cause difficulties in accurate estimation of elastic modulus of thin films.[7,9] In some cases, these problems are somewhat circumvented by testing the bulk gel. It is, however, likely that the elastic properties of bulk gels are different from their counterparts as thin films. We report in this paper that the recently developed buckling based metrology technique[10] is quite suitable for the estimation of the modulus of thin sol−gel films.

The adhesion promoting sol−gel film of interest here is the Boegel EPII formulation developed by The Boeing Company.[11] Development of Boegel EPII was fueled by the increasing concern of the environmental effects of the traditionally used chromate conversion coatings,[12] which are potentially toxic. The system is based on a dilute aqueous solution of zirconium and epoxy functionalized silicon alkoxides, details of which are described in refs 11 and 13. The alkoxides are first hydrolyzed in solution so that they react with the hydroxyl groups on the metal surface through condensation reactions. The organic functional groups are chosen such that they are compatible with the adhesive. The glycidoxy functional group is ideally suited to react with the amine functionalized cross-linker used in epoxy systems. In between the metal and organic resin the Boegel film forms a hybrid organic−inorganic coating through cross-linking condensation reactions (Figure 1).

Throughout the rest of this paper, we will refer to Boegel EPII simply as sol−gel. The major advantage of the Boegel EPII formulation is its ability to cure at room temperature, which allows its easy processing on tempered aluminum parts used in airplane manufacturing. At this low temperature cure, however, it is likely that the sol−gel film is not fully cross-linked; residual hydroxyl groups may remain. Previous studies in our lab using a model epoxy adhesive elucidated that the fracture energies of the sol−gel reinforced joints are strong functions of the curing history[13,15] in both dry and wet and environments. This suggests that the performance of the sol−gel is a function of the degree of cross-linking within the film. It is expected that a fully cured sol−gel film should impart higher adhesion strength and hydrolytic stability compared to an incompletely cross-linked film provided that the excessive curing of a sol−gel film does not degrade the chemical functional groups. This issue can become quite complex, as a number of system parameters may play their roles in a conflicting manner. Our main objective in the current study is to characterize the modulus of the sol−gel film as a function of different curing parameters in order to gain some understanding of the mechanical properties of these films.

When a thin rigid film adhered to a softer elastic substrate is exposed to an external stress, the surface can buckle due to the mismatch of strain in the adjacent layers. As each layer tries to obtain a minimum energy state due to compression and bending, the surface buckles to minimize the overall energy of the system (Figure 2).

The classical approach to solving this problem of relating the buckling wavelength to the material parameters is based on a force[16] or an energy[17−19] balancing method. For a semi-infinite

*To whom correspondence should be addressed. E-mail: jol304@lehigh.edu.

 Published on Web 07/20/2010

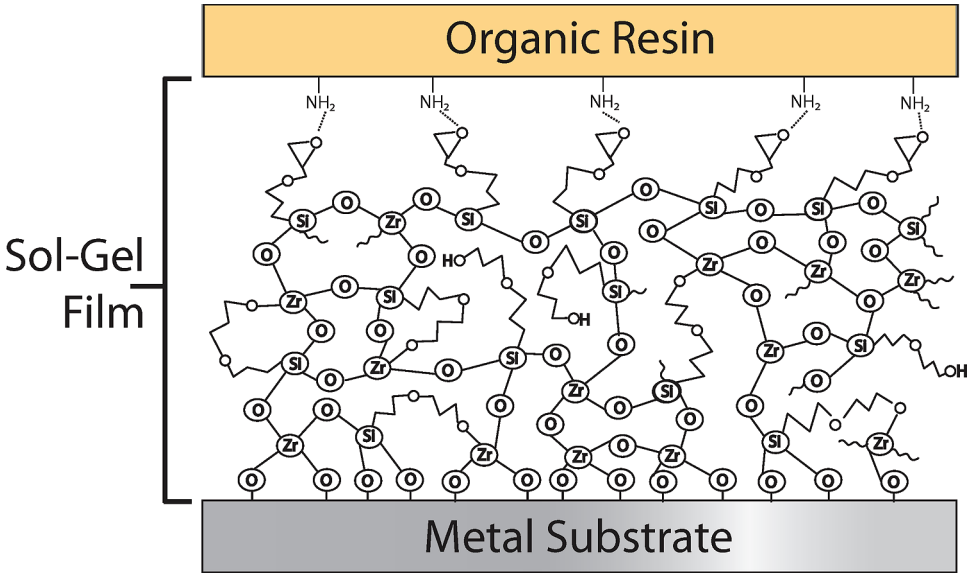

Figure 1. Schematic of Sol−gel coating for adhesion promotion adapted from reference Liu2006. Coating is generated from an aqueous sol of Glycidoxypropyltrimethoxysilane (GTMS) and Zirconium tetrapropoxide (TPOZ). XPS studies[14] show the sol−gel/metal interface to be rich in zirconium and the sol−gel/organic resin interface to be silane rich.

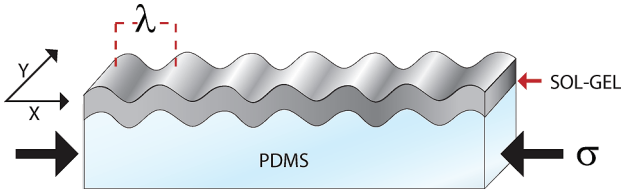

Figure 2. Schematic of the buckling of a thin sol−gel layer on a soft compliant PDMS substrate. When a compressive stress (σ) is applied to PDMS, buckles appear perpendicular to this force. The buckling wavelength λ is a function of the plane strain moduli of the two materials and the thickness of the sol−gel layer.

substrate, i.e., when its thickness is much larger than the thin coating, the wavelength of the buckling instability can be given by eq 1:

$$\lambda = 2\pi h_{SG}\left[\frac{(1-\nu_{PDMS}{}^2)E_{SG}}{3(1-\nu_{SG}{}^2)E_{PDMS}}\right]^{1/3} \quad (1)$$

where E_{SG}, E_{PDMS}, ν_{SG}, ν_{PDMS}, h_{SG}, and λ are the elastic modulus of the sol−gel layer, elastic modulus of the PDMS, the Poisson ratio of the sol−gel, the Poisson ratio of the PDMS, the thickness of the sol−gel film, and the buckling wavelength, respectively. In this work, we are primarily interested in the relative change of the modulus of the sol−gel film as a function of different curing parameters. Given this interest and that the Poisson's ratio of the sol−gel film is an uncertain parameter, we will present the data in terms of the plain strain modulus, which is defined as

$$\bar{E}_{SG} = \frac{E_{SG}}{(1-\nu_{SG}{}^2)}$$

Equation 1 can then be rearranged to solve for the plain strain modulus of the sol−gel film. Where elastic modulus is required, for comparison to the literature, we have estimated the value assuming a range of suitable Poisson ratios.

This buckling instability has been studied in detail for a wide variety of systems such as thin metallic films and silica type layers on PDMS.[20−22] The general method used to achieve the above goal[10,22] is now commonly referred to as the strain induced elastic buckling instability for mechanical measurement (SIEBIMM). In this regard the most studied system is the buckling of polystyrene films on PDMS substrates, although the modulus of several other polymers, polyelectrolytes, and dielectric films have also been determined using this method.[10,23,24] In this paper we apply the buckling instability technique to determine the elastic modulus of a sol−gel film under various conditions.

A roadmap of this paper is as follows. After the description of the Experimental Section, we present data showing that the wavelength of the buckling instability of the sol−gel film varies linearly with its thickness in its fully cured state. This initial part of the study demonstrates that the relationship between the wavelength and the thickness of the sol−gel film is quite robust, this allows us to estimate the modulus of the film either from the gradient of their linear correlation or from a single measurement of wavelength for a given film thickness. The former method can be used when the property of the film does not change as a function of thickness. However, we are bound here to make measurements from a single set of data in many cases, where the properties of the incompletely cross-linked films are likely to depend on its thickness. Using the measurements of the latter kind, we present data showing how the modulus of the sol−gel film depends on the curing temperature. These data allow a correlation to be made between the modulus and the adhesive performance of the film when it is used as a thin film adhesion promoter for the adhesion of epoxy to aluminum. Being encouraged by these findings, we extend the scope of this study to incorporate the dependence of other variables, such as the duration of cure of the sol−gel films and the effect of humidity on its properties. The paper then ends with a discussion on the relevance of these studies and a conclusion.

Experimental Section

Preparation of the Sol−Gel Solution. Details on the formulation of the sol−gel solution can be found in the literature.[11,13] Here, we present only a brief summary. The sol−gel films are formed from a dilute aqueous solution of Glycidoxypropyltrimethoxysilane (GTMS) (97% Gelest), Zirconium tetrapropoxide (TPOZ) (70% w/w in *n*-propanol, Alfa Aesar), glacial acetic acid (Sigma-Aldrich), and Antarox BL-240 (Rhodia Inc.). The thickness of the film was controlled by changing the concentration of the GTMS and TPOZ in the sol. Immediately

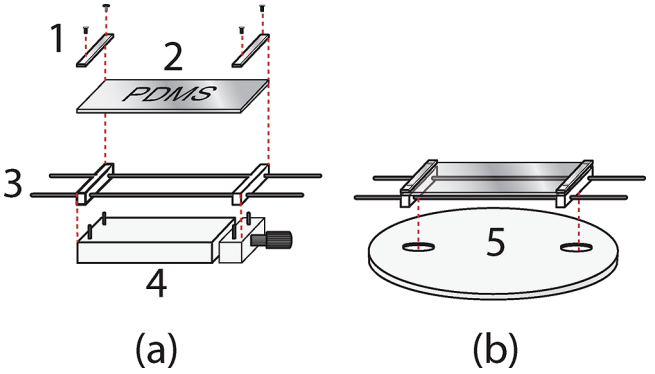

Figure 3. Illustration of sample mount, strain micrometer and spin-coating mount. Mounting brackets (1) are used to firmly secure the PDMS sheet (25 × 75 × 2 mm) (2) to the sample mount (3). The sample mount is then loaded onto the locking pins of the micrometer (4). The distance between the fastening blocks on the sample mount can be easily adjusted to ensure that sufficient prestrain is applied to the PDMS sheet. Locking nuts on the fastening blocks allow this strain to be locked in place. After removing the PDMS loaded sample mount from the micrometer, it was fastened to the spin coating mount (5). After the sol−gel film was spin coated on PDMS, the sample mount was removed from the spin coating mount and placed in the required curing environment. After the required cure had taken place, the sample mount was then reattached to the micrometer where the strain was applied and recorded.

before applying the sol−gel coating to PDMS, it was passed through a 2 μm qualitative filter paper (Whatman). PDMS substrates were coated within 2 h of the preparation of the sol.

Surface Preparation and Modification of PDMS Elastomeric Substrates. Sylgard 184 (Dow Corning) was used as the elastomeric support. Curing agent was mixed thoroughly with the base in the ratio of 1:10. After degassing the mixture for 12 h, the mixture was cured at 65 °C for 4 h in a convection oven (Tenny Jr., Thermal Product Solutions), in the form of thin (2 mm) sheets. These sheets are cut into coupons measuring 25 mm ×75 mm. After loading them to a sample holder, as described in the next section, they were washed with DI water and blown dry with nitrogen. The sample mount is then placed on a conductive surface and exposed to the corona generated from a Tesla coil for 1 min. This treatment produces a thin silica like layer, which is wettable by water (contact angle of $< 5°$). These surfaces do reconstruct slowly; hence they have been used within 3 min after coronal treatment. Bowden et al[25] have studied the effect with PDMS exposed to oxygen plasma, and conjectured that increasing the exposure time to plasma increases the silica layer thickness. In the present study, the low energy corona discharge is used for a short duration in order to oxidize the surface that minimizes the formation of a thin silica-like layer. The difference of the elastic modulus between this thin silica type layer and the bulk PDMS itself causes surface buckling upon application of a compressive stress. The silica type layer, created from the corona treatment, and its effect on the measured sol−gel buckling wavelength is addressed in the start of the Results and Discussion.

Coating of Sol−Gel Film on PDMS Substrates, Testing Procedure, and the Determination of Film Thickness. A customized apparatus (Figure 3) was designed for surface modification, spin coating, and application of controlled strains to the PDMS samples. This design avoids the need to remove the PDMS from the sample holder, which eliminates unwanted stress causing film delamination. The PDMS was securely fastened to the sample mount and then prestressed to minimize any sagging of the film during the spin coating process (Figure 3a). The amount of strain in the sample was recorded from the micrometer reading. After securing the sample mount in this position and removing it from the micrometer, the surface of PDMS was exposed to corona discharge as described above.

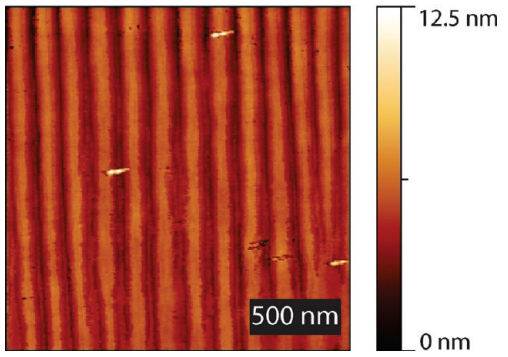

Figure 4. AFM scan of a PDMS surface treated with a corona discharge buckling under an applied strain. PDMS surfaces are exposed to a corona discharge for 1 min under ambient conditions, 23 °C and 47% RH, subjected to a strain of ~8%.

Next it was mounted onto the spin coater (Headway Instruments) after attaching it to a spin coating plate (Figure 3b). Sol−gel solution was applied to the PDMS with a pipet and allowed to thoroughly wet it for 2 min. Samples were spun at 1200 rpm for 50 s, then cured either at the ambient condition or inside a convection oven.

For the samples cured at temperatures above 75 °C, the thermal expansion provides a level of strain that is sufficient to cause buckling in the film. The wavelength of the buckling is independent of the applied strain provided that it is low enough, i.e., $< 10\%$. For other samples, strains of ~1.5−4% were applied to the system by relaxing the prestressed PDMS. Buckling wavelength was estimated by imaging three areas on the substrates selected at random. Images were taken using either an optical microscope in a reflectance mode (Nikon) or with an atomic force microscope (Nanodimension V) when the buckling wavelength is below ~2 μm.

The thickness of the sol−gel films on PDMS was determined with a scanning electron-microscope (Hitachi 4300). Typically, the thicknesses of the thin films on PDMS are analyzed[23,24] using variable angle spectroscopic ellipsometry (VASE). While the through put rate with the SEM analysis is not as high as the VASE, it has the advantage that the film thickness can be clearly visualized on the substrate and that the measurements can be made in absolute scale. Samples were cut with a scalpel and mounted in such a way that the film thickness is perpendicular to the field of view. Samples were then sputtered with Iridium for 10 s (Electron Microscopy Sciences EMS 575x). The thickness of the film was determined from the SEM images using an image analysis software at a number of positions along the interface. As a separate study, the thicknesses of the sol−gel films deposited on silicon wafers were determined with ellipsometry (Rudolph Research AutoEL III).

Results and Discussion

Estimation of the Properties of the Silica Type Layer. Oxidation of the surface of PDMS causes the formation of a thin silica-like layer. The mismatch in elastic moduli of this film and that of the bulk PDMS causes the surface to buckle when a compressive stress is applied. Bowden et al[25] have found that the buckling wavelength increases with oxidation time, suggesting that the thickness of this stiff layer also increases. In the aforementioned work oxygen plasma is used to modify the surface of PDMS. In the present study a corona discharge was used to oxidize the surface of PDMS, as outlined in the Experimental Section. Although this treatment is lower in energy than oxygen plasma, it must still be assumed that a thin film is formed on the surface of PDMS. When this treated surface is strained above ~8%, small buckles can be seen on the surface (Figure 4).

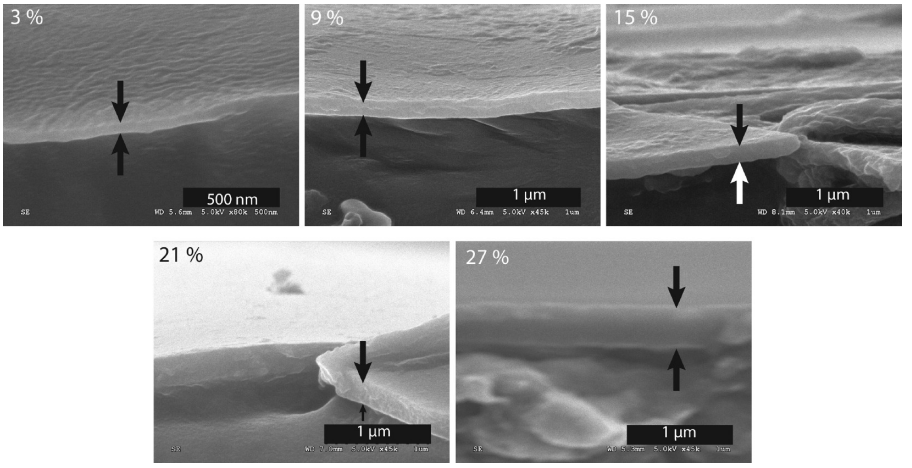

Figure 5. SEM micrographs showing the thickness of the sol−gel film on PDMS films for five different sol−gel concentrations. Concentrations are displayed in the upper right corner of each image. Samples were cut with a scalpel and mounted on a SEM stub such that the PDMS/sol−gel interface was at 90° to the electron gun. Note the change of scale on the images.

The presence of these buckles indicates that a silica type layer is formed on the surface due to the corona exposure, which could affect the measurements of the properties of the sol−gel films deposited on it. The surface bucklings on the oxidized PDMS have an amplitude and wavelength of ~2.2 nm and ~0.18 μm respectively (Figure 4) at ~8% strain. In order to make an estimate as to what extent the measurements could be affected, let us compare the bending rigidities of the corona generated silica layer on PDMS and that of the most weakly cross-linked sol−gel films in our studies. We can combine the standard expression for the flexural rigidity of an elastic plate with eq 1 as follows

$$D_{Silica} = \frac{\bar{E}_{Silica} h_{Silica}^{3}}{12} = \frac{\bar{E}_{PDMS}}{4}\left(\frac{\lambda}{2\pi}\right)^{3}$$

where E_{Silica} and h_{Silica} are the plane strain modulus and thickness of the silica layer respectivaly. Using the wavelength of the buckling of the oxidized PDMS (~0.18 μm), a value of the flexural rigidity of the silica-like layer is estimated as $D_{silica} = 1.6 \times 10^{-17}$ N m. By comparison, the flexural rigidity of a thin (50 nm) weakly cross-linked sol−gel film of an elastic modulus of 2 MPa and Poisson's ratio of 0.25 is $D_{solgel} = 2.2 \times 10^{-17}$ N m. As these bending rigidities are very close to each other, we expect the silica layer to have a significant effect on the determination of the elastic property of the weakly cross-linked and very thin sol−gel film. In this paper, however, the modulii of the sol−gel films for the vast majority of cases are significantly higher than 2 MPa with the corresponding flexural rigidities orders of magnitude larger than that of the corona generated thin oxide layer on PDMS.

Estimation of the Elastic Modulus of the Sol−Gel Films. In order to validate the method of buckling instability to estimate the properties of the sol−gel films, the effects of the concentration of the sol−gel precursor on the thickness and the elastic modulus of the resultant film were evaluated. A curing temperature of 120 °C was chosen in order to avoid the degradation of the GTMS component[26] of the sol−gel film that could occur at a higher temperature. This is also a reasonably high temperature at which the film is cured completely. Figure 5 displays the SEM images of the sol−gel films from which their thicknesses were measured. Figure 6 compares the thicknesses of the sol−gel films measured using the above method with those of the films deposited on a

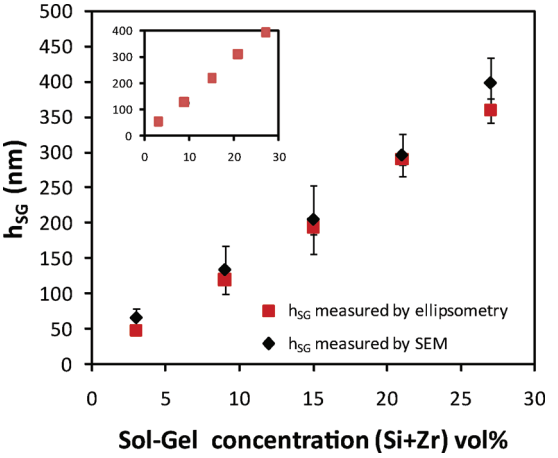

Figure 6. Comparison of film thickness (h_{SG}) vs sol−gel concentration measured via two different techniques. Black diamonds correspond to SEM measurements for the sol−gel films cured at 120 °C on a PDMS support and the red squares correspond to the ellipsometry measurements for films cured under indentical conditions on silicon wafer. Insert: Ellipsometry results for the thickness of films cured under ambient conditions (23 °C and 47% RH) for 24 h as a function of sol−gel concentration. On average, the oven cured films show an ~8% decrease in thickness compared to the room temperature cured. Error bars are hidden in the marker size.

silicon wafer under similar conditions using the method of ellipsometry. This comparison shows that both methods yield similar results. We use the thickness measured by SEM in these studies for the convenience of measurements done on PDMS rubber; it also provides the measurements to be done in absolute scale.

Figure 7 shows that the thickness of the sol−gel film as well as the buckling wavelength increases linearly with the concentration of the starting sol precursor. From here onward, all the data will be presented as a function of the thickness of the sol−gel film instead of the sol concentration. Figure 8 summarizes the buckling wavelength vs film thickness data for sol−gel films cured at 120 °C. From the gradient of the line passing through the experimental points, its plane strain modulus is estimated to be 1.7 ± 0.2 GPa. In the same figure, the plane strain modulus of each film as estimated using eq 1 is reported. As expected, these values closely cluster around their mean. On the basis of this obvious comparison, we conclude that either method can

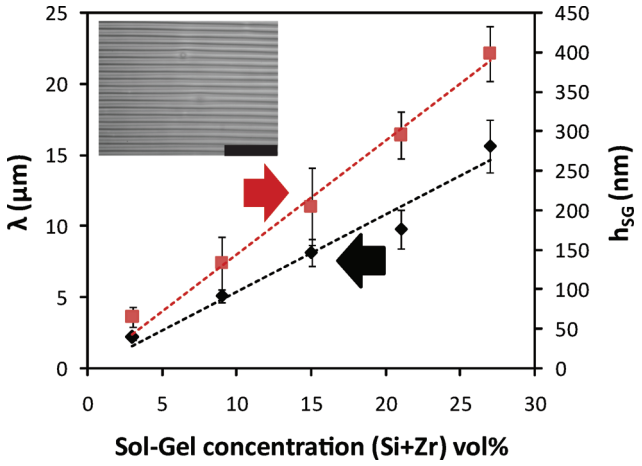

Figure 7. Effect of sol concentration ((Zr + Si) vol %) on film thickness (h_{SG}) and buckling wavelength (λ). Black diamonds represent the buckling wavelength vs sol−gel concentration whereas the red squares represent sol−gel film thickness (as measured by SEM) vs sol−gel concentration. A linear relationship is observed in the buckling wavelength vs sol−gel concentration. Here, the buckling wavelength was measured using optical microscopy for films cast from sol−gel concentrations equal to and above 9 vol %. AFM was used for measuring the wavelength of films formed from sol−gel concentrations below 9 vol %. Error bars represent one standard deviation of the data. Sol−gel films were cured at 120 °C. Inset: Optical microscopy image of buckling on a film cast from a sol−gel concentration of 7 (Si + Zr) vol %. Scale bar represents 50 μm.

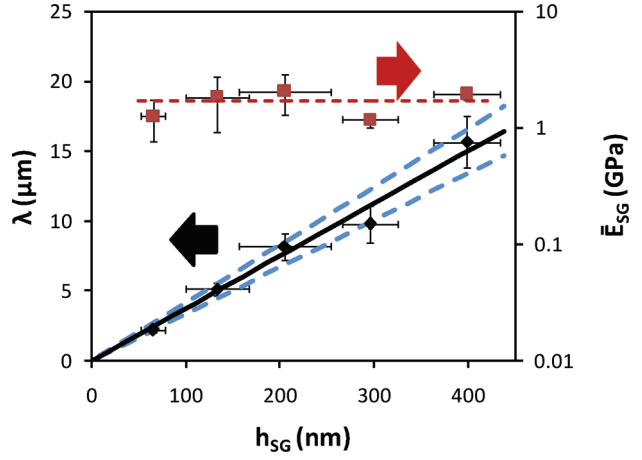

Figure 8. Relation of buckling wavelength (λ) and plane-strain modulus (E_{SG}) to sol−gel film thickness (h_{SG}). Film thickness is measured via SEM. Wavelength data displayed in Figure 7 are replotted against film thickness. Using the data in Figure 7 it is shown here that the plane-strain modulus is independent of film thickness. Black diamonds represent buckling wavelength vs sol−gel film thickness, whereas the red squares represent the modulus of the sol−gel thin film. The black line represents a line of best fit on the buckle wavelength vs film thickness data which passes through the origin. The blue dashed lines represent 95% confidence intervals on the buckle wavelength vs film thickness results.

be used to accurately determine the elastic modulus of the sol−gel film. It can be seen from this figure that the largest error in the data and indeed the major limit of accuracy of the technique is the measurement of the thickness of the film. The statistical error is comparable to those of other techniques such as nanoindentation and three point bending tests (for bulk gels).

As the properties of a sol−gel film strongly depend on its chemical formulation and curing history, it is difficult to

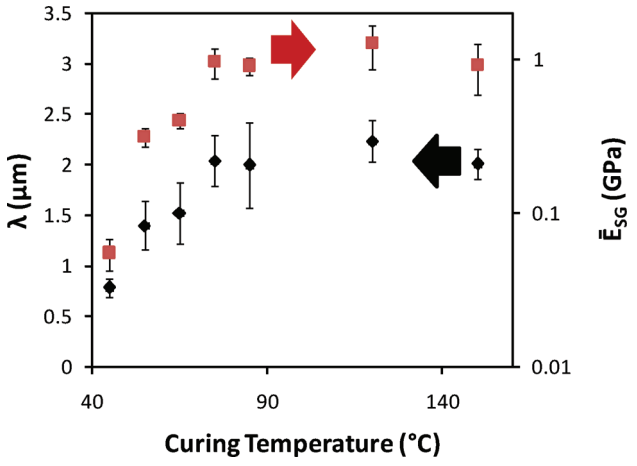

Figure 9. Buckling wavelength (λ) and plane-strain modulus (E_{SG}) as a function of curing temperature. Plane-strain modulus is calculated from the displayed wavelength. Cure time was 30 min at approximately 47% RH. Black diamonds represent the buckling wavelength vs sol−gel film curing temperature, whereas the red squares represent sol−gel thin film modulus vs sol−gel film thickness.

compare our results to any similar results published in the literature. Nevertheless, it is instructive to look at two particular examples. However, before this comparison is made it is necessary to define a suitable Poisson's ratio for the sol−gel film in order to convert the plane-strain modulus to the elastic modulus. It is difficult to ascertain the exact value of the Poisson's ratio for this film as it contains both organic and inorganic components. Thus, we used an approximate method. Poisson's ratio for mesoporous silica films[27] is reported to be 0.25, while that for amorphous polymeric solids[28] is in the range of 0.3−0.4. Given the above values of the Poisson's ratio we used a range of 0.25−0.35 to estimate the elastic modulus of the sol−gel film. The elastic modulus of the film cured at 120 °C is then estimated to be in the range of 1.5 to 1.6 GPa. Atanaciao et al[7] reported the moduli of various organic−inorganic hybrid films based on the mixtures of TEOS (tetraethoxysilane) and alkyltriethoxysilanes of various kinds as obtained using nanoindentation. Of particular relevance here is that of the TEOS and GTMS formulation. The Young's modulus of this film was found to be around 1.68 and 1.81 GPa when measured on silicon and copper substrates, respectively.[7] In a separate study, bulk gels of TEOS + GTMS + TPOZ have been investigated using Knoop microindentation for which the elastic modulus was estimated to be around 0.57 GPa when the gels were cured at 125 °C for 72 h.[8] The value of the modulus of the sol−gel films estimated by us fall in between those reported in the above two studies, although direct comparison cannot be made.

The Effect of the Curing Temperature on the Modulus of the Sol−Gel Films. The curing temperature of the sol−gel based coating is an important contributor to the final strength of the adhesive joint. It is generally believed that the coating needs to be cured to a degree that does not affect the ability of primers or adhesives to wet and penetrate it to some extent so that a defect free interface can be formed. Figure 9 shows that the curing temperature has a pronounced effect on the modulus of the thin (65 ± 13 nm) sol−gel films. The modulus, and thus the cross-linking density, of the film sharply increases with the curing temperature until all the major cross-links are formed leading to a plateau in modulus. The exact nature of these cross-links is, however, unclear although silicon−oxygen−silicon, zirconium−oxygen−zirconium, zirconium−oxygen−silicon, and silicon−oxygen−substrate, and zirconium−oxygen−substrate are all possible. The epoxy ring of GTMS can also open to form a

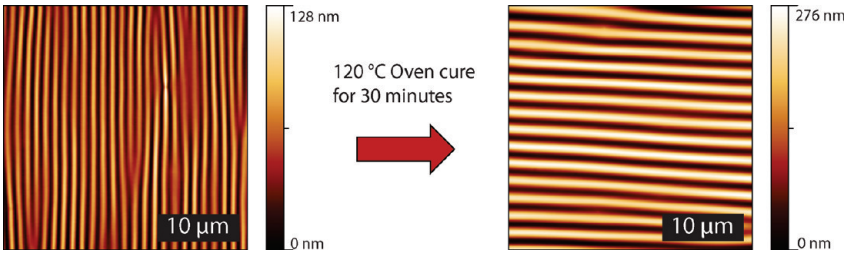

Figure 10. AFM images of the effect of post curing a film after it is aged under ambient conditions for 2 days. The left image shows the buckling wavelength of the film after aging it under ambient conditions (23 °C, 47% RH) for 2 days. The right image shows the effect of post curing this sample at 120 °C for 30 min. The wavelength changes from ~1.1 μm to ~2 μm. This causes a change in plane strain modulus from 0.2 ± 0.03 to 1 ± 0.3 GPa. If the sol−gel film (65 nm thick) is cured directly at 120 °C for 30 min the estimated plane strain modulus is 1.3 ± 0.4 GPa. Buckles for oven cured films are orientated perpendicular to those at room temperature as the buckling is caused by the thermal stress. Thermal stress generates one-dimensional buckling due to the geometric confinement of the clamp, this effect is described in detail in the text.

diol but it is unclear whether these functional groups are involved in any cross-linking reaction. The specific cross-links aside, nearly a 17-fold rise in elastic modulus occurs when the curing temperature is increased from 45 to 85 °C. It is assumed that within the range of temperature used in these studies, the maximum possible degree of cross-linking is achieved at the above temperature. This result coincides with the previously reported[26]IR spectroscopy studies with the GTMS films, which found that no significant change in the degree of condensation occurs within a curing temperature range of 93−180 °C. The previously mentioned ellipsometric studies (Figure 6) on film thickness show a ~8% decrease in film thickness between room temperature cure and 120 °C cured films. This decrease is within the statistical variation in the SEM thickness measurement and as such is not directly measurable. However, it is worthwhile to note that this decrease in thickness would accentuate the trend of elastic modulus with curing temperature which we observe here.

The compressive strain required for buckling can be generated either by an externally applied force or due to the stresses developed in the film due to the mismatch of thermal expansion coefficients during a thermal curing cycle. As noted in the Experimental Section, sol−gel films cured below 75 °C were buckled mechanically by releasing the prestrained PDMS substrate. Films cured above 75 °C buckled due to thermally induced stress. It is important here to consider a potential artifact in the estimation of the modulus of thin films which arises due to thermal stress. The modulus of a thin polymer brush, in which buckling was induced by thermal stress, is about four times lower than when the buckling was induced mechanically.[23] Should a similar effect be present in our system, elastic modulus at room temperature of the thermally buckled sol−gel films would be higher than our current estimation. This would accentuate the trend that the elastic modulus increases with curing temperature.

It is worthwhile to note that if the film is cured at 120 °C after aging it for 2 days at room temperature (23 °C) it shows the increase in the modulus (Figure 10) of the film that is comparable to that cured directly at 120 °C. This effect is discussed further later in the paper.

This change of modulus suggests that the unreacted hydroxyl groups remain within the film that are activated when exposed to higher temperature. This is important for achieving good adhesion with an epoxy or other adhesives that can be post cured on the sol−gel film at higher temperature. We bring up this issue next as we attempt to find a relationship between the modulus of sol−gel coating and its adhesion performance with epoxy under dry and wet conditions.

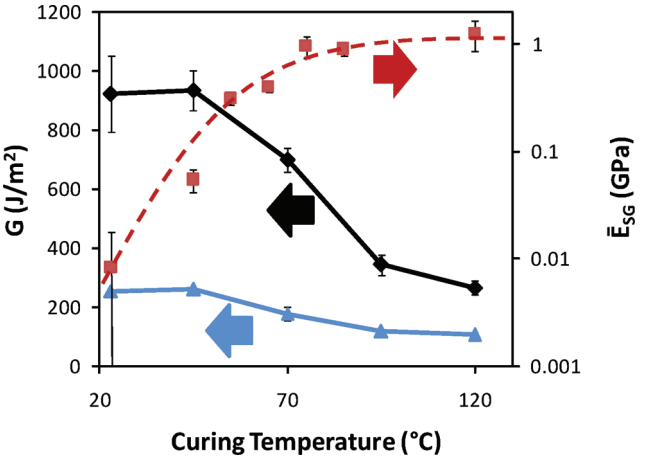

Figure 11. Fracture strength (G) of an aluminum/sol−gel/epoxy joint under wet and dry conditions versus the curing temperature of the sol−gel primer. The plane-strain modulus (E_{SG}) dependence on the curing temperature is replotted from Figure 9 on the right axis. Black diamonds and blue triangles represent dry and wet fracture strengths respectively versus sol−gel curing temperature. Red squares represent the plane-strain modulus versus the curing temperature. Details of the wet vs dry fracture experiments are outlined in the text. The aluminum (2024-T3) substrates are etched in a Forest Products Laboratory solution prior to sol−gel application.[29]

An Empirical Correlation between the Modulus of the Sol−Gel Coating and Its Adhesive Performance. In our laboratory, Liu[29] studied the effect of sol−gel cure temperature on the fracture strength of the aluminum/sol−gel/epoxy joint under wet and dry conditions. The critical energy release rates of these joints were measured using the method of an asymmetric double cantilever beam. Fracture experiments under ambient conditions were carried out at 23 °C and 47% RH, whereas those under wet conditions were conducted by inserting a water droplet into the crack tip for 2 min before extending it with a wedge. Here, we attempt to seek if any correlation exists between the critical fracture strength of the adhesive joints and the elastic modulii of the sol−gel films as found in our experiments. The results summarized in Figure 11 show that the dry joint strength of the adhesive joint decreases considerably with increasing modulus. From this comparison we surmise that increasing the cross-link density of the film, thus increasing its modulus, possibly decreases the interpenetration of the epoxy into the sol−gel layer. The correlation also suggests that this effect is predominant after a critical modulus (50 MPa) is exceeded, above which any further increase in modulus is extremely detrimental to the joint. The wet strength results show a similar trend as well, although the effect of the modulus of the sol−gel film is less

prominent here. The fact that the lower cross-linked sol−gel films display superior joint strength under both dry and wet conditions suggest that the sol−gel layer is further cross-linked during the cure of the epoxy adhesive which occurs at 100 °C. As previously mentioned, sol−gel films aged at a low temperature (Figure 10) can be post cured at higher temperatures. This observation suggests the following scenario when they are used as adhesion promoters. The adhesive can diffuse into the low temperature cured sol−gel films and react with the available epoxy groups to some extent. When the adhesive is aged at a temperature of 100 °C, the cross-linking of the sol−gel films also increases, thus allowing the formation of an interpenetrating network. This post cure idea has been previously speculated in the literature and is reviewed nicely by Abel et al.[30] This is of relevance to industrial applications, where it is important to ensure that a surface remains chemically active after pretreatment, as there is often a lag time between surface treatment and adhesive joint preparation.

Having established a strong correlation between the modulus of the sol−gel films and its adhesive performance, we now present some data on how this modulus is affected by the duration of cure and humidity.

Duration of Cure at Room Temperature and the Modulus of the Sol−Gel Films. The previous studies performed in our laboratory[15] show that the highest increase in adhesion occurs when the gel is cured at room temperature for 75 min. In our current study, we do not observe buckling for room temperature cured films until a minimum of 3 h is passed since the coating step. The plane strain modulus of the sol−gel film at this cure time (3 h) is estimated to be 8 MPa. The critical strain (ε_{crit}) for buckling to occur is given by eq 2.

$$\varepsilon_{crit} = \frac{1}{4}\left(\frac{3\bar{E}_{PDMS}}{\bar{E}_{SG}}\right)^{2/3} \quad (2)$$

For a sol−gel film of modulus 8 MPa, eq 2 predicts that the critical strain needs to be about 24% before the buckles are formed. In our experiments, we see buckles even when the sol−gel films are subjected to a strain of 1.5−4%. The single film buckling equation does not describe the formation of the buckles for such films, although the prediction (3% strain) is reasonably good for films aged for 9 h or more (Figure 12). The origin of the above discrepancy is not clear to us. We surmise that the elastic modulus of the sol−gel film is very low at cure times of <3 h under ambient conditions (23 °C, 47% RH), which is not measurable by this technique. Films cured for 24 h under 20% RH at 23 °C gave a plane strain modulus of 200 ± 70 MPa. Compared to the value recorded at 47% RH and 23 °C of plane strain modulus 170 ± 30 MPa we can conclude that lowering the humidity does not have an appreciable effect on the rate of cure of the sol−gel film.

Effect of Humidity on a Post Cured Sol−Gel Thin Film. We now describe the final segment of our study, where we report the effect of humidity on the properties of the sol−gel film. It is well-known that the strength of any adhesive promoted by a sol−gel coating in an humid environment is of paramount importance to various industrial applications. As mentioned above, Liu et al[13,15] investigated the adhesive performance of epoxy/Boegel EPII/aluminum joints under wet conditions. The overall conclusion of these studies is that water decreases the durability of the joint, thus decreasing its threshold fracture energy. Other studies[31−33] show as well that water is capable of penetrating into the adhesive joints and damaging the integrity of the sol−gel film over time by hydrolyzing

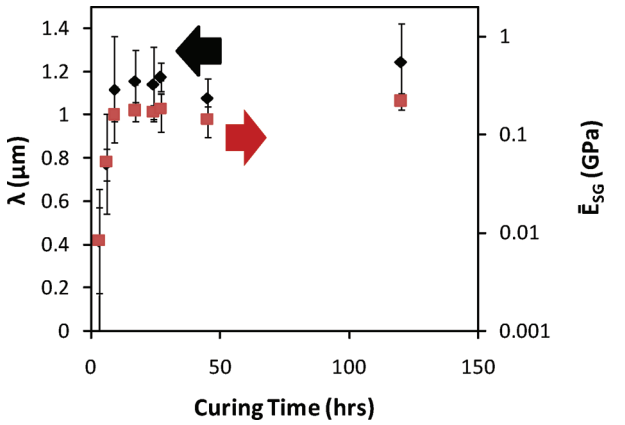

Figure 12. Effect of curing time, under ambient conditions (23 °C, 47% RH), on sol−gel film plane-strain modulus (E_{SG}). A strain of ~3% was applied to induce buckling. The black diamonds represent the buckling wavelength vs curing time, whereas the red squares represent sol−gel thin film modulus vs curing time.

the interface. Polymer films are also known to swell in the presence of many solvents, which induce instabilities within the film or the relaxation of residual stresses.[17,23] With these facts in mind, weinvestigate the effects of humidity on the behavior of buckled sol−gel films.

Figure 13 depicts the effect of humidity on the morphology of the buckled sol−gel coatings when they are stored under ~98% RH (relative humidity) for 15 h. A number of intriguing pattern formations are evident. The change in the buckling pattern when the films are cured at low temperatures (45−65 °C) and then exposed to high humidity is different from those cured at higher temperatures (85−150 °C) and stored under similar conditions. It is important here to clarify a point made briefly in the Experimental Section. When cured at temperatures below 75 °C, the films do not buckle upon removal from the oven. Buckling is induced by releasing the prestrain in the PDMS; therefore, the compressive strain is applied in the x direction (see Figure 2). This results in the formation of buckles parallel to the y coordinate. For samples cured at temperatures above 75 °C, we observe buckling upon cooling due to the mismatch in the thermal expansion coefficients of the sol−gel coating and PDMS. The buckling however is oriented parallel to the x coordinate. This 90° rotation in the buckling pattern can be explained by considering the way in which the PDMS expands in the metal clamp. As Figure 3 shows, the PDMS is securely clamped at both ends. During the heating process, the film is free to expand in the y direction anywhere other than near the clamps where it is constrained. The prestrain in the x direction is chosen to ensure that the thermal expansion does not cause sagging of the PDMS. Were it not for this confined geometry, buckles in the herringbone or labyrinth conformation should occur as a result of thermal stress.[20] Upon cooling the PDMS, contractions in the y direction generate a compressive force within the cured sol−gel layer. This results in the formation of buckles orientated perpendicular to this force.

Films cured at 85−150 °C show neither any significant change in the buckling wavelength in the x direction (see Figures 13 and 14) nor in their amplitude (Figures 13 and 15) when they are placed in the humid environment. Were the elastic modulus or film thickness to change as a result of exposure to high moisture, the ratio of the buckling wavelength at high humidity to that of ambient should also change. One would also expect a decrease in the buckling amplitude. Figures 14 and 15, however, show that these

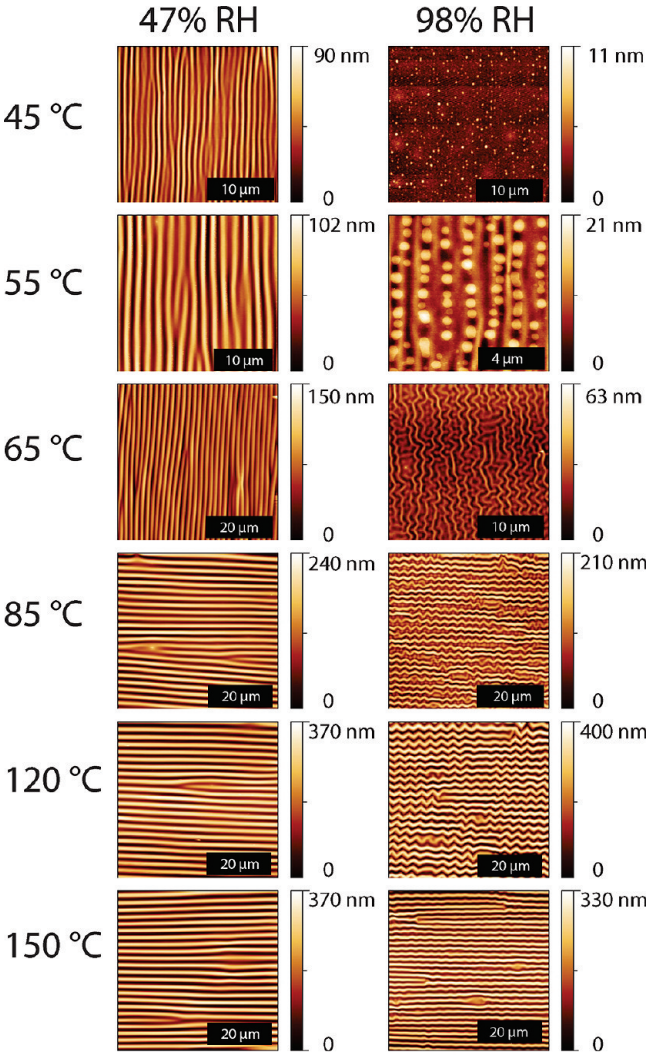

Figure 13. AFM scans showing the effect of humidity on oven cured sol−gel films (65 nm). The curing temperatures are as shown in the figure. The left column shows the buckling morphology observed after the oven cure for 85−150 °C cured films exposed to ambient humidity (~47% RH). The right column shows the subsequent change in the surface morphology after being exposed to a high humidity (~98% RH) environment for 15 h. Note the change of scale between images.

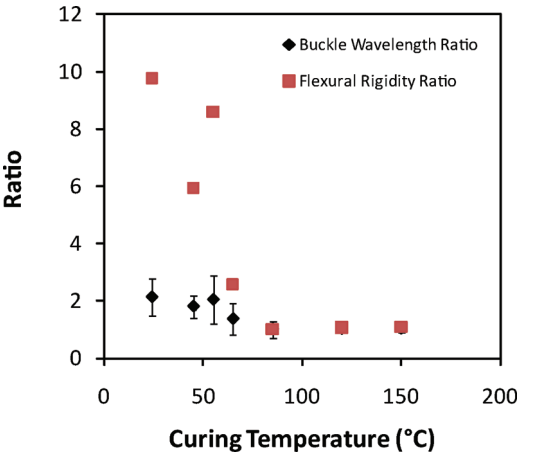

Figure 14. Ratio of the buckling wavelength and ratio of the sol−gel flexural rigidity before exposure to high humidity (RH ~ 98%, for 15 h) to that measured after exposure as a function of curing temperature. Black diamonds represent the ratio of the buckling wavelength. Red squares represent the ratio of the sol−gel film flexural rigidity. A ratio greater than 1 indicates a decrease in wavelength and flexural rigidity due to high humidity exposure. Films cured under ambient conditions (23 °C and RH ~ 47%) were cured for 24 h. All other temperature cure times were 30 min.

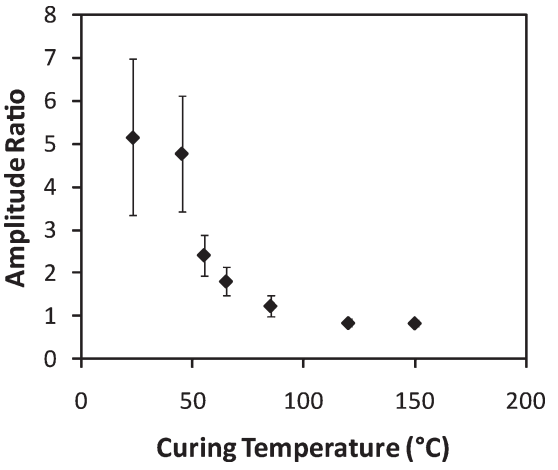

Figure 15. Ratio of the buckling amplitude before exposure to high humidity (RH ~ 98%) for 15 h to that measured after exposure as a function of curing temperature. A ratio greater than 1 indicates a decrease in amplitude due to high humidity exposure. Films cured under ambient conditions (23 °C and RH ~ 47%) were cured for 24 h. All other temperature cure times were 30 min.

ratios are constant, indicating that films cured above 85 °C undergo a minimal level of swelling in humid environment. Nevertheless, a definite change in the buckling morphology occurs in humid atmosphere, indicating that water is able to penetrate into the film and thus modify its stress state. The 1 D buckling pattern evolves to a classical herringbone buckling pattern. This is characterized by the development of kinks on the original buckles. The formation of this herringbone pattern implies that the compressive stress in the x direction increases above the critical stress for surface instability. Recent simulations by Huang et al[34] suggest that similar patterns can be formed on membranes subject to a mismatch of stress. These simulations further show that as the anisotropy of the stress state is increased, the buckling morphology goes through 3 major transitions: labyrinth to herringbone to the one-dimensional mode. We observe a similar trend in the change in humidity driven buckling between films cured at 65 °C and above. Films cured at 65 °C appear to display a hybrid labyrinth−herringbone conformation upon exposure to humidity whereas films cured above 85 °C display herringbone buckles. Our results also coincide with the experimental data presented recently by Lin and Yang,[35] who studied the formation of herringbone and labyrinth morphologies on surface-oxidized PDMS. These experiments investigated the effect of a biaxial stress condition, either sequentially or simultaneously, on the buckling morphology. Herringbone patterns are formed by sequentially applying the biaxial stresses. Labyrinth patterns are formed with the simultaneous application of biaxial stress. In our studies, the kinks do not appear uniformly throughout the film cured at 150 °C, whereas for films cured at 65 and 85 °C the kinks are uniform across the sample area. Comparison of our results with the simulation[32] and experimental results[35] implies that an increase in the compressive stress generated through a resistance to swelling could be responsible for these buckling transitions. Films cured at higher temperatures are subject to a higher stress

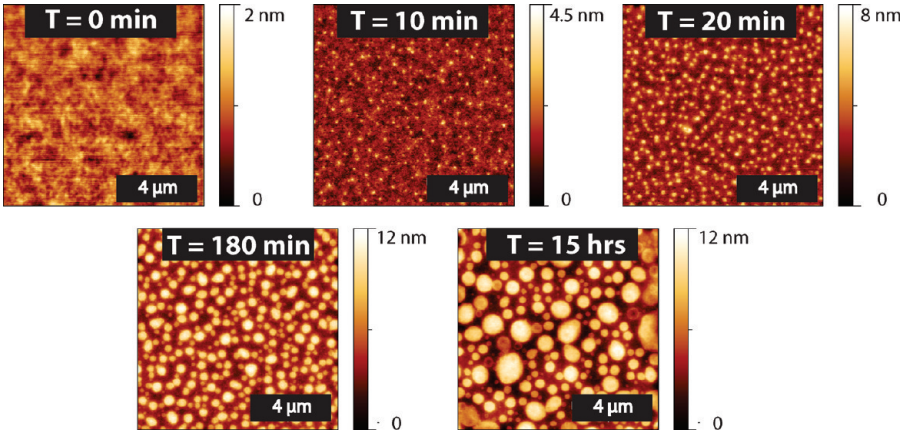

Figure 16. AFM scans show the morphological evolution of storing an unbuckled 65 nm thick sol−gel film on PDMS at ~98% RH. These films were cured at 55 °C for 30 min under ambient humidity (~47% RH) before exposure to ~98% RH. No blisters develop before $T = 10$ min.

upon cooling. Therefore, the transition in the buckling states with increase in temperature could be due to a higher initial 1D buckling stress with higher cure temperature or an increase in the swelling stress from increased moisture penetration.

The effect of moisture on the lower temperature (23, 45, and 55 °C) cured films is more complex. For these temperature cures, the amplitude of the buckles decreases significantly upon exposure to high humidity (Figure 15) and in some cases it becomes difficult to observe them on the surface. Films cured at 45 °C and room temperature show a small decrease in amplitude when stored under ambient conditions, ~10−20%, however this is small compared to the decrease observed in the humid environment (a 5-fold decrease). This decrease under ambient conditions suggests that the sol−gel film is able to creep to relax the stress. Creep in low temperature cured GTMS based sol−gel films has also been observed by Atanaciao et al.[7] eq 3 relates the amplitude of the buckles to the system parameters.

$$A = h\sqrt{\frac{\varepsilon_{pre}}{\varepsilon_{crit}} - 1} \tag{3}$$

Here ε_{pre} is the prestrain and ε_{crit} is defined in eq 2. Assuming that the thickness increases due to swelling and the prestrain remains more or less constant (interfacial slip is minimized) then the decrease in amplitude must occur due to the increase of the critical strain. In order for critical strain to increase, the elastic modulus of the sol−gel must decrease. Therefore, it is likely that the penetration of water in to the sol−gel layer reduces the elastic modulus. It appears that the humid environment is capable of swelling the film and thus relaxing the stress. Water vapor appears to have the opposite effect on the films cured at higher temperatures owing to their higher cross-linking density compared tothose cured at lower temperatures.

The relaxation of the amplitude of the buckled sol−gel films cured at low temperature is one of two types of morphological changes that occur upon exposure to a high humidity environment. The second morphological change is dictated by the level of strain applied to the sample to induce buckling prior to humid exposure. We will first deal with the effect of storing films buckled initially under ~1.5% strain. For films cured at 23, 45, and 55 °C and buckled under 1.5% strain, droplets are formed on the surface after storage in a humid environment. This effect is also observed occasionally on the films cured at 65 °C. In order to better understand the

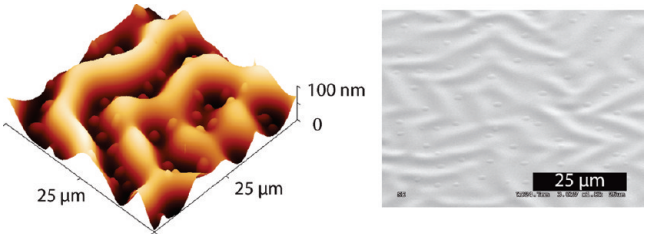

Figure 17. AFM (left) and SEM (right) images show the effect of storing a 300 nm thick sol−gel films coated on PDMS at ~98% RH for 15 h The films were cured at 55 °C for 30 min at ambient humidity (47%) before exposing to the ~98% RH atmosphere. The humidity causes the surface to buckle and blisters to form. The blisters preferentially lie in the valleys of the buckles.

origin of these surface features, the growth kinetics of the droplets were studied in the unbuckled state on PDMS substrates (Figure 16). Dewetting of the sol−gel layer as a cause of these features was ruled out as no definitive long-range order of the droplets was found via Fourier image analysis. Furthermore, the rate of increase of the size of the droplets (Figure 16) is much too high for it to be attributed to the subsequent Ostwald ripening of the dewetted droplets. The height (5 nm) of the droplets is an order of magnitude smaller than the film thickness. The effect of storing sol−gel coated glass substrates, cured at 55 °C and at a high humidity (~98%) was also studied. No droplets are observed on these surfaces after 15 h. This suggests that the droplets arenot a low molecular weight polymer which diffuses to the surface upon humid exposure. It is possible that these droplets are blisters caused by the delamination of the sol−gel film from the PDMS surface.

Films as thin as 300 nm were also studied in order to discern the effect of film thickness on droplet formation. These films coated on PDMS were stored under ~98% humidity for 15 h in the unbuckled state. While the droplets on the 65 nm thick film could not be observed due to their small vertical height (5 nm), they were readily visible in the SEM (Figure 17) on the 300 nm thick films. This 300 nm thick film also exhibits buckling after exposure to ~98% RH humidity, the pattern of which corresponds to an isotropic stress state.

Numerous blistering patterns, from circular to telephone cord,[36] have been widely reported in the literature and are comprehensively reviewed by Hutchinson and Suo.[37] The blisters observed in our experiments lie preferentially in the valleys of the buckles with an orientation parallel to the

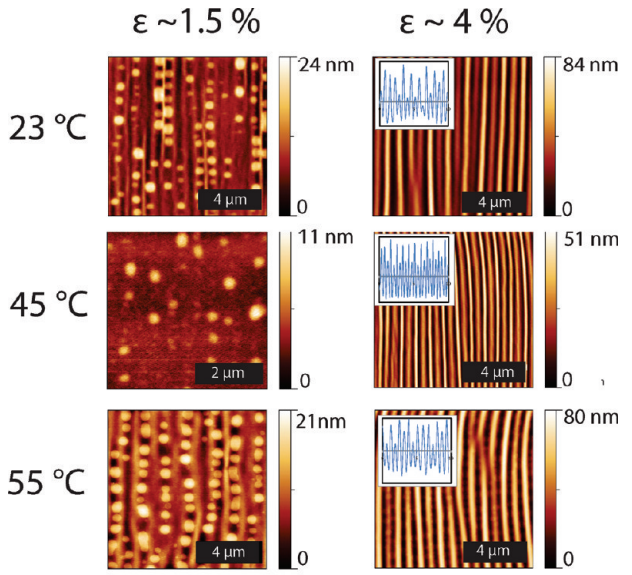

Figure 18. Effect of prestrain on the change in buckling morphology due to the storage of buckled sol−gel films in humid environments (~98% RH, for 15 h). Prestrains are shown at the top of the figure. Films buckled at $\varepsilon \sim 1.5\%$ display circular blisters on exposure to high humidity. Films buckled at $\varepsilon \sim 4\%$ show a decrease in buckle wavelength. Inset: Line profiles of the films after humid exposure which were initially buckled under and $\varepsilon \sim 4\%$.

direction of the buckles. Figure 16 shows that the blister size increases with storage time, which is consistent with solvent induced blistering phenomena in thin films.[38] Interestingly, these droplets differ in one significant way to the blisters in the previously mentioned work,[38] in that the vast majority of the blisters in our case do not collapse upon removal from the solvent environment. The blisters also remain in the sample after it has been stored in a vacuum for 48 h. The presence of these blisters in the SEM image shown in Figure 17 also illustrates their stability under vacuum. This is counter to the typical blisters, which collapse after the external stress is released.

Mei et al.[39] investigated the effect of simultaneous surface buckling and blister formation in thin film systems. Both phenomena have a characteristic critical stress below which they do not occur. They found that whether or not a film buckles or blisters depends on the ratio of the substrate to the film elastic moduli and the ratio of the width of delamination to the film thickness. For a fixed size of the debonded region, a low ratio of elastic moduli ($E_{substrate}/E_{film}$) favors surface buckling, whereas a high ratio favors the formation of blisters. As previously mentioned, the change in buckle amplitude for films cured at and below 65 °C due to exposure to high humidity (98% RH) suggests a decrease in the elastic modulus (Figure 15). This raises the value of the substrate to film elastic modulus ratio and thus it is possible that the critical stress for blister formation is surpassed. It is also possible that the influx of water into the film could increase the size of the debonded region by attacking the chemical bonds at the surface. The increase in the size of the debonded region would also lower the critical stress required for blister formation.

At higher strain levels, ~4%, a different change in surface morphology is observed. Figure 14 shows approximately an 8 fold change in the flexural rigidity for films cured at 23 °C, 45 °C, and 55 °C upon exposure to high humidity. This corresponds to a 2 fold decrease in the wavelength due to the humid exposure. Closer inspection of these buckles in certain

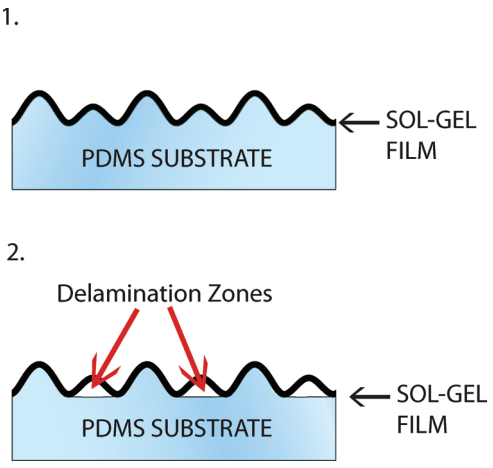

Figure 19. Schematic of secondary buckle evolution in sol−gel films cured at low temperature < 55 °C as a result of humid exposure. Case one is where the film remains adhered to the PDMS substrate. Case two is where the sol−gel film delaminates from the PDMS to form straight sided blisters.

regions reveals some interesting profiles as shown in Figure 18. It is observed from these profiles that the amplitude of the buckles increases and decreases in a regular pattern across the profile for the room cured and 45 °C cured samples. This effect of alternating amplitude is uniform over the 45 °C cured samples whereas for room cured and 55 °C cured samples, some variation exists. The reason for this variation is not clear. Two possibilities exist for these secondary buckles, i.e. either the sol−gel film is delaminated from the surface forming a straight sided blister or remains adhered to the PDMS substrate (Figure19).

It is not possible to state which is the actual case at this time. However, we conjecture that these secondary buckles are blisters formed by the delamination of the sol−gel from the substrate due to the influx of water. The multiple blisters observed for films stored at a lower strain strengthen this argument as it is well documented that straight sided blisters can become unstable and break up into small circular blisters.[40] This helps to explain the ordering of the blisters along the buckle directions on the surface. It is possible that some interesting surface patterning techniques could be developed using this methodology.

From the above discussion, it is clear that the simultaneous buckling and delamination of the sol−gel films under humid atmosphere is a complex situation. Irrespective of the exact nature and formation of the blisters on the sol−gel surface, it can be reasoned that exposure to a humid environment has a greater effect on films cured at and below 65 °C than those cured above it.

Summary and Conclusion

The elastic modulus of a sol−gel based adhesion promoting film has been estimated using the method of buckling instability. For a sol−gel curing temperature of 120 °C, the plane strain modulus of the film is independent of the film thickness and estimated to be 1.7 ± 0.2 GPa. From this result and accounting for the uncertainty in the Poisson's ratio we estimate the elastic modulus to be in the range of 1.5−1.6 GPa. This value is consistent with literature values for similar sol−gel based films. The technique was used to characterize the modulus as a function of sol−gel curing history and also to qualitatively describe the effect of moisture on the film. Elastic modulus was found to be a strong function of curing temperature up to curing temperatures of 85 °C. Increasing the cure temperature above this value does

not yield any substantial change in elastic modulus. Room temperature cured films displayed no buckling at cure times below 3 h. A plateau in modulus was reached at curetimes above 9 h. Change in the buckling morphology due to exposure to high humidity suggests that the lower the film cure temperature the more susceptible it is to moisture penetration and swelling. The presence of the hydroxyl groups in the imperfectly cross-linked film appear to facilitate the influx of water. The higher the water concentration the greater the expected driving force for the cleavage of cross-links via hydrolysis;[41] so the films cured at lower temperatures are more susceptible to hydrolytic attack than their high temperature cure counterparts. Thus, the low temperature films should perform poorly in wet adhesion experiments. As this is not the observed trend (Figure 11), it provides further weight to the argument that the sol−gel film undergoes further cross-linking during the epoxy cure cycle. These results call for a study to be conducted using a room temperature cure epoxy to determine the importance of the adhesive cure step. The buckling technique presented here would be of great use in such a study as the temperature effect on film cross-linking can be studied in detail alongside a qualitative assessment of the film moisture resistance.

Acknowledgment. This work was supported by Lehigh University and The Boeing Company. We would like to acknowledge D. H. Berry, J. E. Seebergh, J. H. Osborne, and K. Y. Blohowiak of Boeing for their helpful discussions.

Note Added after ASAP Publication. This article posted ASAP on July 20, 2010. The references have been revised. The correct version posted on July 26, 2010.

References and Notes

(1) Plueddemann, E. P. *Silane Coupling Agents*, 1st ed.; Plenum Press: New York, 1982.
(2) Brinker, C. J.; Scherer, G. W. *Sol-Gel Science: The Physics and Chemistry of Sol-Gel Processing*, 1st ed.; Academic Press: San Diego, CA, 1990.
(3) Chaudhury, M. K.; Pocius, A. V. *Surfaces, Chemistry & Applications*, 1st ed.; Elsevier: Amsterdam, 2002.
(4) Zheludkevich, M. L.; Salvado, I. M.; Ferreira, M. G. S. *J. Mater. Chem.* **2005**, *15*, 5099–5111.
(5) Hoebbell, D.; Nacken, M.; Schmidt, H. *J. Sol-Gel Sci. Technol.* **2000**, *19*, 305–309.
(6) Hoebbell, D.; Nacken, M.; Schmidt, H. *J. Sol-Gel Sci. Technol.* **2001**, *21*, 177–187.
(7) Atanacio, A. J.; Latella, B. A.; Barbe, C. J.; Swain, M. V. *Surf. Coatings Technol.* **2005**, *192*, 354–364.
(8) Innocenzi, P.; Esposto, M.; Maddalena, A. *J. Sol-Gel Sci. Technol.* **2001**, *20*, 293–301.
(9) VanLandingham, M. R.; Villarrubia, J. S.; Guthrie, W. F.; Meyers, G. F. *Macromol. Symp.* **2001**, *167*, 15–43.
(10) Stafford, C. M.; Harrison, C.; Beers, K. L.; Karim, A.; Amis, E. J.; VanLandingham, M. R.; Kim, H.-C.; Volksen, W.; Miller, R. D.; Simonyi, E. E. *Nat. Mater.* **2004**, *3*, 545–550.
(11) Blohowiak, K. Y.; Osborne, J. H.; Krienke, K. A. US Patents5,814,137, 5,849,110, 5,939,197, and 6,037,060, 1996−1998.
(12) Du, Y. J.; Damron, M.; Tang, G.; Zheng, H.; Chu, C.-J.; Osborne, J. H. *Prog. Org. Coat.* **2001**, *41*, 226–232.
(13) Liu, J.; Chaudhury, M. K.; Berry, D. H.; Seebergh, J. E.; Osborne, J. H.; Blohowiak, K. Y. *J. Adhes. Sci. Technol.* **2006**, *20*, 277–305.
(14) Greegor, R. B.; Blohowiak, K. Y.; Osborne, J. H.; Krienke, K. A.; Cherian, J. T.; Lytle, F. W. *J. Sol-Gel Sci. Technol.* **2001**, *20*, 35–50.
(15) Liu, J.; Chaudhury, M. K.; Berry, D. H.; Seebergh, J. E.; Osborne, J. H.; Blohowiak, K. Y. *J. Adhes. Sci. Technol.* **2008**, *22*, 1159–1180.
(16) Allen, H. G. *Analysis and Design of Structural Sandwich Panels*; Pergamon: New York, 1969.
(17) Genzer, J.; Groenewold, J. *Soft Matter* **2006**, *2*, 310–323.
(18) Groenewold, J. *Physica A* **2001**, *298*, 32–45.
(19) Cerda, E.; Mahadevan, L. *Phys. Rev. Lett.* **2003**, *90*, Art No. 074302.
(20) Bowden, N.; Brittain, S.; Evans, A. G.; Hutchinson, J. W.; Whitesides, G. M. *Nature* **1998**, *393*, 146–149.
(21) Chan, E. P.; Crosby, A. J. *Soft Matter* **2006**, *2*, 324–328.
(22) Volynskii, A. L.; Bazhenov, S.; Lebedeva, O. V.; Bakeev, N. F. *J. Mater. Sci.* **2000**, *35*, 547–554.
(23) Huang, H.; Chung, J. Y.; Nolte, A. J.; Stafford, C. M. *Chem. Mater.* **2007**, *19*, 6555–6560.
(24) Nolte, A. J.; Rubner, M. F.; Cohen, R. E. *Macromolecules* **2005**, *38*, 5367–5370.
(25) Bowden, N.; Huck, W. T. S.; Paul, K. E.; Whitesides, G. M. *Appl. Phys. Lett.* **1999**, *75*, 2557–2559.
(26) Bertelsen, C. M.; Boerio, F. J. *Prog. Org. Coat.* **2001**, *41*, 239–246.
(27) Tsai, C.-T.; Lu, H.-Y.; Ting, C.-Y.; Wu, W.-F.; Wan, B.-Z. *Thin Solid Films* **2009**, *517*, 2039–2043.
(28) Brown, D.; Clarke, J. H. R. *Macromolecules* **1991**, *24*, 2075–2082.
(29) Liu, J. Ph.D. thesis, Lehigh University, 2006.
(30) Abel, M. L.; Allington, R. D.; Digby, R. P.; Porritt, N.; Shaw, S. J.; Watts, J. F. *Int. J. Adhes. Adhes.* **2006**, *26*, 2–15.
(31) Abel, M. L.; Adams, A. N. N.; Kinloch, A. J.; Shaw, S. J.; Watts, J. F. *Int. J. Adhes. Adhes.* **2006**, *26*, 50–61.
(32) Kinloch, A. J.; Korenberg, C. F.; Tan, K. T.; Watts, J. F. *J. Mater. Sci.* **2007**, *42*, 6353–6370.
(33) Chaudhury, M. K.; Gentle, T. M.; Plueddemann, E. P. *J. Adhes. Sci. Technol.* **1987**, *1*, 29–38.
(34) Huang, Z. Y.; Hong, W.; Suo, Z. *J. Mech. Phys. Solids* **2005**, *53*, 2101–2118.
(35) Lin, P.-C.; Yang, S. *Appl. Phys. Lett.* **2007**, *90*, 241903.
(36) Thouless, M. D. *J. Am. Ceram. Soc.* **1993**, *76*, 2936–2938.
(37) Hutchinson, J. W.; Suo, Z. *Adv. Appl. Mech.* **1991**, *29*, 63–191.
(38) Sharp, J. S.; Jones, R. A. L. *Phys. Rev. E* **2002**, *66*, 011801.
(39) Mei, H.; Huang, R.; Chung, J. Y.; Stafford, C. M.; Yu, H.-H. *Appl. Phys. Lett.* **2007**, *90*, 151902.
(40) Parry, G.; Coupeau, C.; Colin, J.; Cimetiere, A.; Grilhe, J. *Acta Mater.* **2004**, *52*, 3959–3966.
(41) Benkoski, J. J.; Kramer, E. J.; Yim, H.; Kent, M. S.; Hall, J. *Langmuir* **2004**, *20*, 3246–3258.